

## Abundance and Reactivity of Dibenzodioxocins in Softwood Lignin

DIMITRIS S. ARGYROPOULOS,<sup>\*,†,‡</sup> LUBO JURASEK,<sup>†</sup> LÍVIA KRIŠTOFOVÁ,<sup>‡</sup>  
 ZHICHENG XIA,<sup>§</sup> YUJUN SUN,<sup>†,‡</sup> AND ERNEST PALUS<sup>‡</sup>

Department of Chemistry, Pulp and Paper Research Centre, McGill University, 3420 University Street,  
 Montreal, Quebec, Canada H3A 2A7, and Paprican, 570 Boulevard St-Jean, Pointe-Claire,  
 Quebec, Canada H9R 3J9

To define the abundance and comprehend the reactivity of dibenzodioxocins in lignin, model compound studies, specific degradation experiments on milled wood lignin, and molecular modeling calculations have been performed. Quantitative <sup>31</sup>P NMR measurements of the increase of biphenolic hydroxyl groups formed after a series of alkaline degradations in the presence of hydrosulfide anions (kraft conditions) showed the presence of 3.7 dibenzodioxocin rings/100 C9 units in milled wood lignin. The DFRC degradation protocol (Derivatization Followed by Reductive Cleavage) was chosen as an independent means to estimate their abundance. Initial experiments with a dibenzodioxocin model compound, *trans*-6,7-dihydro-7-(4-hydroxy-3-methoxyphenyl)-4,9-dimethoxy-2,11-dipropyldibenzo[*e,g*]-[1,4]dioxocin-6-ylmethanol, showed that it is not cleaved under DFRC conditions, but rather it isomerizes into a cyclic oxepine structure. Steric effects precluded this isomerization from occurring when DFRC was applied to milled wood lignin. Instead, monoacetylated biphenolic moieties were released and quantified by <sup>31</sup>P NMR, at 4.3 dibenzodioxocin rings/100 C9 units. The dibenzodioxocin content in residual lignins isolated from kraft pulps delignified to various degrees showed that during pulp delignification, the initial rate of dibenzodioxocin removal was considerably greater than the cleavage rate of arylglycerol- $\beta$ -aryl ether bonds. The activation energy for the degradation of dibenzodioxocins under kraft conditions in milled wood lignin was  $96 \pm 9$  kJ/mol, similar to that of arylglycerol- $\beta$ -aryl ether bond cleavage.

**KEYWORDS:** 5,5'-Biphenyl; activation energy; derivatization followed by reductive cleavage (DFRC); dibenzodioxocin; HMBC; HMQC; model compound; kraft pulping; lignin; NMR; <sup>31</sup>P; <sup>13</sup>C; oxepine

### INTRODUCTION

Lignin is an aromatic biopolymer that constitutes ~30% of the dry weight of softwoods and ~20% of the weight of hardwoods (1). The structure of native lignin cannot be fully characterized because of the difficulty of isolating native lignin from the plant cell walls. Milled wood lignin is considered to be the most representative lignin preparation (2, 3). Chemically, lignin is built from phenylpropanoid units linked together by various bonds.  $\beta$ -O-4-coupling of a monolignol with the growing lignin polymer creates the most abundant structural unit in softwood lignin, the  $\beta$ -aryl ether. Because ~50% of the phenylpropanoid units in lignin are involved in  $\beta$ -O-4-structures, the cleavage of these bonds is essential for delignification (4). Reactions of lignin and lignin model compounds under pulping conditions have been studied extensively (5, 6). Phenylcoumaran

( $\beta$ -5) structural units with 9–12% of total phenylpropanoid units are also prominent in softwood lignins (7). The proportion of phenylpropanoid units in biphenyl structures in softwoods ranges from 19 to 26% (8–10). The percentage of free biphenolic hydroxyl groups obtained by quantitative NMR spectroscopy is 5–8%, which indicates that the biphenyl structures in softwood lignins are etherified to a large extent (10–12).

In 1995, Brunow's group discovered that the majority of the *o,o*-dihydroxybiphenyl structures are etherified with phenylpropanoid units in lignin as eight-membered ring dibenzodioxocin structures (13, 14). Dibenzodioxocins are now proposed to be the main branching points in softwood lignin (13).

During the past decade lignin structural inquiries have been greatly facilitated by the development of various degradative protocols, such as hydrogenolysis (1), acidolysis (15), thioacidolysis (16), and DFRC (Derivatization Followed by Reductive Cleavage) (17). Nondegradative protocols, such as NMR, have also been used. DFRC, which efficiently cleaves the  $\alpha$ - and  $\beta$ -aryl ethers in lignins, releasing analyzable monomers for quantification, is a powerful degradative method developed recently by Lu and Ralph (17). The DFRC method uses different

\* Corresponding author [telephone (514) 398-6178; fax (514) 398-8254; e-mail dimitris.argyropoulos@mcgill.ca].

<sup>†</sup> Department of Chemistry, Pulp and Paper Research Centre, McGill University.

<sup>‡</sup> Paprican.

<sup>§</sup> Department of Chemistry, McGill University.

chemistry for ether cleavage and is therefore a useful alternative to the solvolytic methods. In a recent publication, the combination of DFRC with quantitative  $^{31}\text{P}$  NMR was shown to have significant potential for the determination of arylglycerol- $\beta$ -aryl ether and other linkages in lignins (18).

The presence of dibenzodioxocins in wood may have serious implications with respect to the reactivity of lignin during wood pulping and biodegradation and possibly during pulp bleaching. In this respect it is crucial to have a protocol for the determination of these units in lignin and to accurately determine their abundance. With this objective we examined the reactivity of dibenzodioxocins in models and within lignin and have arrived at an estimate for their abundance and propose a protocol for their determination.

## MATERIALS AND METHODS

**Materials.** Acetyl bromide (Eastman Kodak Co.), acetic anhydride 99% (J. T. Baker), ammonium chloride 99% (BDH Inc.), glacial acetic acid (99.7%), zinc dust (97.4%), dioxane (99.9%), methylene chloride (99.99%), ethyl acetate (99.9%), and orthophosphoric acid (85%) were purchased from Fisher Scientific. 3,4-Dimethoxytoluene (96%), used as an internal standard in HPLC quantifications, 2-chloro-4,4,5,5-tetramethyl-1,3,2-dioxaphospholane (95%), used as a phosphorylation reagent, cholesterol, used as an internal standard for  $^{31}\text{P}$  NMR spectra (99+%), sodium hydroxide (99.99%), and sodium sulfide nonahydrate (99.99%) were all purchased from Aldrich. The water used in this study was first distilled and then passed through a NANO Pure analytical deionization system (Barnstead).

**Synthesis of Dibenzodioxocin Model Compound 1.** (1) *Catalytic Hydrogenation of Isoeugenol.* Isoeugenol (50 g) was dissolved in 200 mL of absolute ethanol, and 0.5 g of 10 wt % Pd/C was added. The reaction was carried out in a 1 L PARR (high-pressure) reactor at room temperature with an initial hydrogen pressure of 3.5 atm. After 1 h, the palladium on charcoal powder was filtered off and the filtrate evaporated to give propylguaiacol as a homogeneous oil in nearly quantitative yield.

(2) *Dimerization of Propylguaiacol.* Sodium acetate ( $\text{CH}_3\text{COONa}$ ; 18.0 g) dissolved in 100 mL of deionized water was placed into a 2 L three-neck flask equipped with a magnetic stirrer. Propylguaiacol (16.8 g) was then added to the solution, and the total volume of water was adjusted to 1 L. Potassium ferricyanide [ $\text{K}_3\text{Fe}(\text{CN})_6$ ; 1.72 g] dissolved in 300 mL of deionized water was then added dropwise to the reaction mixture under vigorous stirring. Stirring was continued at room temperature for 24 h. At the end of reaction, 200 mL of dichloromethane was added into the reaction flask. The water layer was extracted three times with methylene chloride (200, 100, and 100 mL). The combined organic layers were washed with a saturated solution of sodium chloride (NaCl), dried with sodium sulfate ( $\text{Na}_2\text{SO}_4$ ), and filtered, and finally the methylene chloride was evaporated under reduced pressure. The raw reaction product was purified by column chromatography [300 g of silica gel, 130–260 mesh, 2 L of solvent (eluent = dichloromethane/acetic acid 100:0.5) (yield = 60%):  $\delta_{\text{H}}$  (200 MHz;  $\text{CDCl}_3$ ) 0.93 (6H, t,  $\text{CH}_3$ ), 1.62 (4H, m,  $\text{CH}_2$ ), 2.52 (4H, t,  $\text{CH}_2$ ), 3.85 (6H, s,  $\text{OCH}_3$ ), 6.69 (2H, s, ArH), and 6.80 (2H, s, ArH) (23).

**Oxidative coupling of dehydrodipropylguaiacol and coniferyl alcohol** was performed according to the published method (14) to produce the required dibenzodioxocin **1** in 35% yield:  $\delta_{\text{H}}$  (200 MHz;  $\text{CDCl}_3$ ) 0.99 (6H, m,  $\text{CH}_3$ ), 1.67 (4H, m,  $\text{CH}_2$ ), 2.64 (4H, m,  $\text{CH}_2$ ), 3.40–3.64 (2H, m,  $\gamma$ - $\text{CH}_2$ ), 3.75, 3.88, 3.92 (3H, s,  $\text{OCH}_3$ ), 4.14 (1H, m,  $\beta$ -H), 4.55 (1H, d, J12.4,  $\alpha$ -H), 5.69 (1H, s, ArOH), and 6.75–6.89 (7H, m, Ar-H).

**Treatment of 1 under Kraft Pulping Conditions.** A white liquor solution was prepared, which contained 1.55 g of sodium sulfide ( $\text{Na}_2\text{S} \cdot 9\text{H}_2\text{O}$ ) and 1.75 g of sodium hydroxide (NaOH) per 50 mL of deionized water.

The pulping experiments were performed in Teflon-lined 5 mL steel bombs with white liquor. Model compound **1** (3 mg) and white liquor (4 mL) were mixed within the bomb, and the air was replaced by nitrogen before sealing. The bomb was then heated in an oil bath for

different lengths of time at 120, 140, and 160 °C. After cooling, the reaction mixture was neutralized with dilute  $\text{H}_3\text{PO}_4$  (0.5 M) and freeze-dried. After lyophilization, a known amount of an internal standard was added and the product extracted with ethyl acetate. Samples for HPLC analyses were withdrawn and filtered (Waters Sep-Pak cartridges). The amounts of released biphenyl **6** and unreacted dibenzodioxocin **1** were determined using an internal standard [3,4-dimethoxytoluene (96%; Aldrich)].

**Treatment of Milled Wood Lignin under Kraft Pulping Conditions.** The procedure was similar to that used for the model compound. The softwood milled wood lignin (80 mg) was dissolved in 1.6 mL of white liquor (see above). The reaction was carried out in a 5 mL stainless steel bomb from which the air had been displaced by nitrogen. The bomb was heated in an oil bath for various periods of time at 140 °C. At the end of the reaction period, the bomb was cooled with cold water, and its contents were acidified to pH 2 using dilute hydrochloric acid. The precipitate was collected by centrifugation and washed with acidified water to remove inorganic salts. The precipitated lignin was then freeze-dried and brought to constant weight at room temperature under reduced pressure.

An additional part of degraded lignin was also recovered because it was a water soluble low molecular weight lignin. The water portion was lyophilized and extracted with high-purity unstabilized tetrahydrofuran (5 mL). This step was repeated three times to isolate more lignin from the inorganic salts. All THF portions were then mixed into a preweighed vial and allowed to evaporate at room temperature in a well-ventilated hood (overnight). After evaporation, the residue became a dark brown viscous oil. To obtain powdered lignin, the residue was redissolved in a mixture of dioxane/water (60:40) and freeze-dried. Both water-soluble and precipitated portions of lignins were dissolved in the NMR solvent (pyridine/ $\text{CDCl}_3$ ) and mixed together.

**Treatment of 1 under DFRC Conditions Followed by Alkaline Hydrolysis.** Acetyl bromide in acetic acid (2:8 v/v; 10 mL) was added to dibenzodioxocin **1** (20.1 mg). The reaction mixture was stirred at 50 °C for 3 h. The solvent was then evaporated to dryness under reduced pressure. An aqueous solution of sodium hydroxide (115 mg in 5 mL of water) was added to the residue and stirred at 45–50 °C for 24 h. The mixture was then neutralized with dilute hydrochloric acid to pH ~5 and extracted with methylene chloride (three times, total volume = 20 mL). The combined extracts were evaporated to dryness under reduced pressure. Around 100 mg of NaOH in 3 mL of deionized water was added to the residue and stirred for 24 h at 45–50 °C. The reaction was neutralized by dilute HCl to pH 6, extracted three times with dichloromethane (total volume = 10 mL), dried over  $\text{Na}_2\text{SO}_4$ , and evaporated. The residue was dried in a desiccator for 24 h.

**Treatment of Milled Wood Lignin under DFRC Conditions.** (Step 1) *Acetyl Bromide Derivatization.* Acetyl bromide in acetic acid (1:9 v/v; 12.5 mL) was added to 50 mg of softwood milled wood lignin. The reaction mixture was stirred at 50 °C for 3 h in a clean flask (care for any residual traces of zinc at this point, their presence could induce erroneous quantitative results). The solvent was then evaporated to dryness under reduced pressure.

(Step 2) *Reductive Cleavage.* The above residue was immediately dissolved in the acidic reduction solvent (dioxane/acetic acid/water = 5:4:1 = v/v/v, 12.5 mL). Zinc dust (250 mg) was added, and the mixture was stirred at room temperature for 30 min. The reaction mixture was then quantitatively transferred to a saturated ammonium chloride solution (50 mL) in a separatory funnel using methylene chloride (20 mL). The aqueous layer was extracted with further methylene chloride (2  $\times$  10 mL). The combined extracts were evaporated to dryness under reduced pressure and placed into the desiccator for 24 h. The final acetylation step of the standard DFRC protocol was not carried out so that the released phenols could be determined by  $^{31}\text{P}$  NMR.

**HPLC analyses** were carried out by reversed-phase HPLC using a Supelcosil LC-18 column (250  $\times$  4.6 mm), 5  $\mu\text{m}$ . Acetonitrile/water (pH adjusted to ~5 with  $\text{H}_3\text{PO}_4$ ) 3:1 was used as the mobile phase. The detector wavelength was set at 285 nm, and the flow rate was 1 mL/min. The integrated areas from the chromatograms were compared to determine the response factor. To calculate the amount of released biphenyl and unreacted dibenzodioxocin from the LC chromatograms,

a response factor was determined using 3,4-dimethoxytoluene as an internal standard (IS).

For example, to determine the amount of dibenzodioxocin (DBDO) response factor  $k = \text{wt}(\text{IS})/\text{wt}(\text{DBDO}) \times \text{area}(\text{DBDO})/\text{area}(\text{IS}) = 0.92$

The response factor for 5,5'-biphenyl was found to be 1.007.

To calculate the amount of unreacted dibenzodioxocin in the reaction product the following equation was used:

$$\text{wt of unreacted DBDO} = \text{wt}(\text{IS})/k \times \text{area}(\text{DBDO})/\text{area}(\text{IS})$$

**Quantitative  $^{31}\text{P}$  NMR Analyses.** Lignin samples were analyzed for the content of 5,5'-biphenyl structures using a previously published method (19), the only difference being the internal standard. Cholesterol was used instead of cyclohexanol. The scan delay time was 5 s.

**NMR Analyses.** NMR experiments were carried out on a Varian Mercury-300 using 15 mg of sample in 0.5 mL of  $\text{CDCl}_3$  in a 5 mm tube. Proton gradient COSY spectra were recorded in an absolute value mode using 128 increments in the F1 dimension with two scans per increment. A phase sensitive gradient [ $^1\text{H}$ ,  $^{13}\text{C}$ ] HMQC and an absolute-value gradient [ $^1\text{H}$ ,  $^{13}\text{C}$ ] HMBC were collected with 200 and 400 increments, respectively, with four repetitions per increment for HMQC spectra and eight for HMBC spectra. For all 2D experiments the relaxation delays were set to be 1 s, and the data size for acquisition was 1K. For phase sensitive experiments, an optimized Gaussian apodization was applied before FT, and for absolute value experiments a squared sine bell function was applied. A typical spectral window for the proton dimension was 2330 Hz and for carbon, 18760 Hz.

**Computational Analyses.** The heats of reactions and partial charges for the compounds were computed with HyperChem 5.11 Professional software (HyperCube, Inc.) after energy minimization with MM+ and then PM3 (20, 21). The details of the computational protocol were as described previously (22).

## RESULTS AND DISCUSSION

**Determination of Dibenzodioxocins by Alkaline Hydro-sulfide Degradation.** Karhunen (23) was among the first to study the behavior of dibenzodioxocin model compounds under soda and kraft pulping conditions. Under alkaline conditions ( $\text{NaOH}$ , 140 °C, 3 h) and in the absence of hydrosulfide anions, phenolic dibenzodioxocin model compounds were reported to cleave with the formation of enol ethers, 5,5'-biphenyl and vanillin. Under kraft pulping conditions, however ( $\text{NaOH}-\text{Na}_2\text{S}$ , 140 °C, 3 h), the same models were reported to degrade nearly quantitatively, liberating 80% of 5,5'-biphenyl with no enol ether formation. Experiments in our laboratory confirmed Karhunen's findings; our yield of 5,5'-biphenyl under kraft conditions was somewhat higher than that originally reported (86%). It was thus decided that one may use the demonstrated sensitivity of dibenzodioxocins toward hydrosulfide anions to determine these moieties in softwood lignin (**Scheme 1**). Softwood milled wood lignin (MWL) was subjected to kraft pulping conditions, and the amount of phenolic hydroxyl groups present in 5,5'-biphenyl structures was measured as a function of time by integrating the range 141.7–140.35 ppm in the quantitative  $^{31}\text{P}$  NMR spectra of the degraded lignins (19, 24).

The original amount of 5,5'-biphenyl hydroxyl groups as determined from the quantitative  $^{31}\text{P}$  NMR spectra of the untreated starting MWL was 0.20 mmol/g. After 4 h at 140 °C, this amount was found to increase to a maximum of 0.60 mmol/g (**Figure 1**). From these data, the amount of dibenzodioxocin structures in softwood MWL was calculated as follows: Assuming the molecular weight of C9 units for softwood MWL is 185 g/mol, our analyses showed that up to 7.4/100 C9 of 5,5'-biphenyl structures could be released during kraft pulping. Because each 5,5'-biphenyl unit consists of two

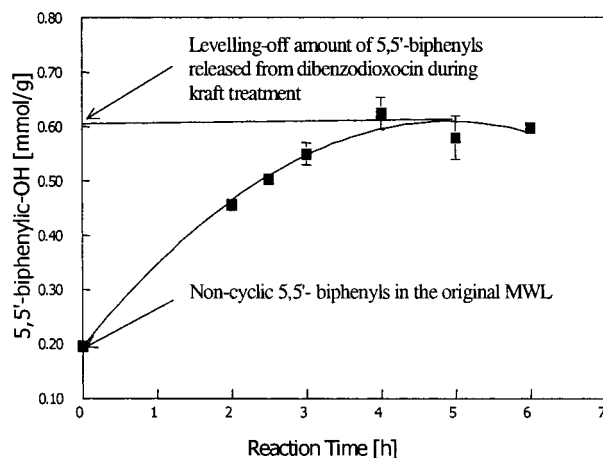
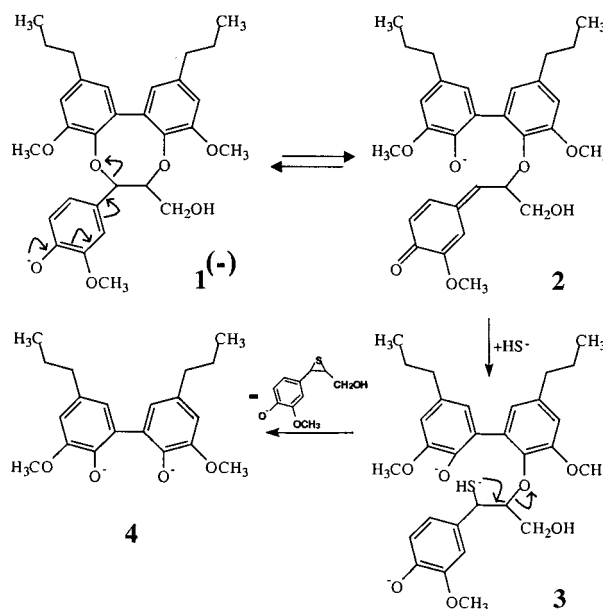


**Figure 1.** Time dependence of concentration of released 5,5'-biphenyl 4 after cleavage of dibenzodioxocin structural unit 1<sup>(-)</sup> within softwood milled wood lignin under kraft pulping conditions at 140 °C.

**Scheme 1.** Proposed Reaction Sequence of Dibenzodioxocin Model Compound 1, Cleavage under Kraft Pulping Conditions Leading to the Formation of a 5,5'-Biphenyl Compound 4

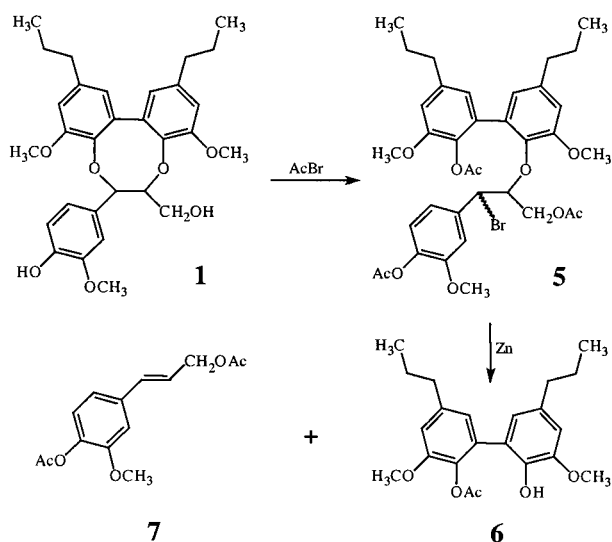


C9 units that contained two phenolic hydroxyl groups, the calculated value needs to be divided by two (per 100 C9 units) and multiplied by three (dibenzodioxocin structure/100 C9 units), because dibenzodioxocin 1 is composed of three C9 units. Therefore, 11.1% of the C9 units are engaged in dibenzodioxocin structures in softwood MWL, and the content of dibenzodioxocin rings in lignin is 3.7/100 C9 units.

**Determination of Dibenzodioxocins Using the DFRC Method.** To confirm our data derived from the alkaline degradation measurements enumerated above, the DFRC method was examined for its feasibility in providing an alternative means for determining these moieties in lignin samples. However, first one needs to comprehend the reactivity of dibenzodioxocins under the conditions dictated by the DFRC protocol.

The DFRC degradation method consists of two steps: (i) bromination and acetylation with acetyl bromide (AcBr) and (ii) reductive cleavage with zinc dust (17). The reaction of lignin with AcBr in acetic acid results in the formation of acetylated  $\alpha$ -bromo derivatives that possess the  $\beta$ -bromo ether skeleton. AcBr in acetic acid at room temperature is highly selective in

**Scheme 2.** Ether Cleavage of Free Phenolic Dibenzodioxocin Model **1** by the DFRC Method



its reactions with lignin; that is,  $\alpha$ -hydroxyls and  $\alpha$ -ethers become  $\alpha$ -bromo derivatives, whereas  $\gamma$ -hydroxyls are acetylated rapidly and phenolic hydroxyls are acetylated more slowly (17). Brominated and acetylated derivatives of lignin models are formed in almost quantitative yields. In the next step the bromoethers are cleaved by reductive elimination with Zn dust to form alkenes. Dibenzodioxocin contains both  $\alpha$ - and  $\beta$ -ether bonds, and it was anticipated that they will react in a manner similar to that of the noncyclic ethers previously described (17).

In our experiments we used *trans*-6,7-dihydro-7-(4-hydroxy-3-methoxyphenyl)-4,9-dimethoxy-2,11-dipropyl-dibenzo[*e,g*]-[1,4]dioxocin-6-ylmethanol, **1**, as a model compound. When the DFRC reaction conditions were applied to **1**, the anticipated release of monoacetylated 5,5'-biphenyl, **6**, and acetylated coniferyl alcohol, **7** (Scheme 2), was not realized. HPLC analyses of the reaction products showed the presence of only

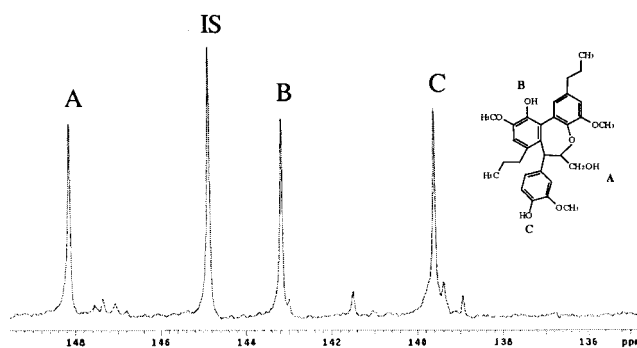


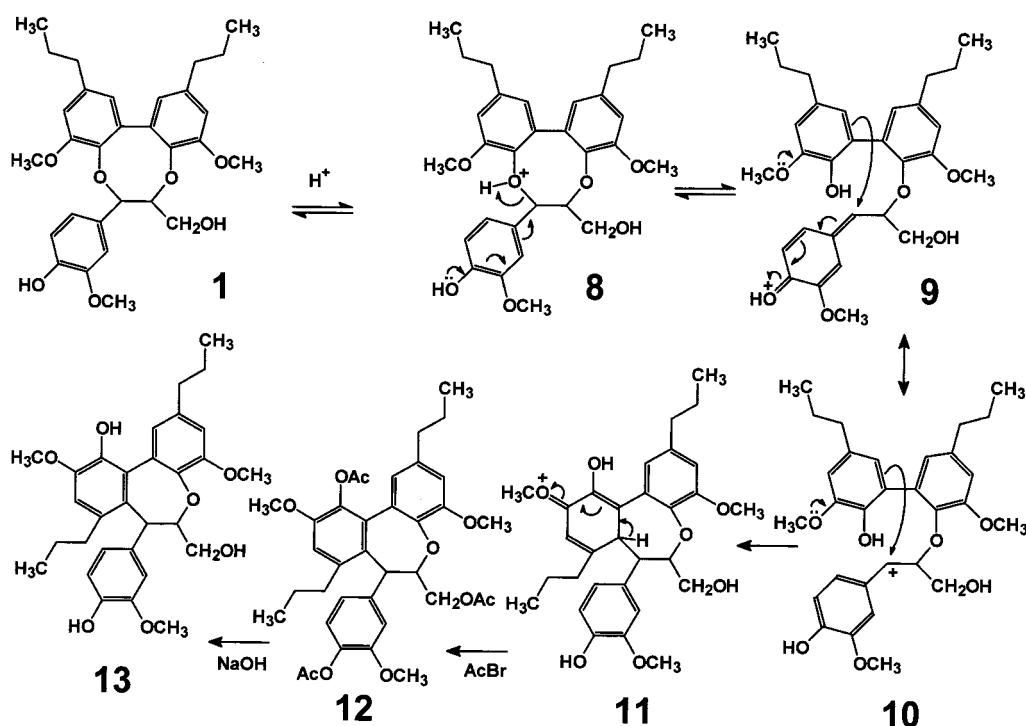
**Figure 2.** <sup>31</sup>P NMR spectrum of the oxepine structure, **13**. The signal marked IS is from the internal standard, cholesterol.

one compound, which did not correspond to any of the expected products. NMR analysis of the compound (Figure 2 and Appendix) proved that it was the oxepine **13** (Scheme 3). The behavior of dibenzodioxocin models under acidic conditions (14, 25) yielding seven-membered ring oxepine structures of considerable stability, accompanied by the release of a single phenolic hydroxyl group, has been documented before. This reaction may account for the release of phenolic hydroxyls that previously have been ascribed to the cleavage of noncyclic benzyl aryl ethers (15). Consequently, the formation of oxepine **13** was not surprising.

As mentioned above, during the acetyl bromide step all free hydroxyl groups are acetylated and only those liberated during the Zn reductive step remain unsubstituted; these can be detected by <sup>31</sup>P NMR. To detect all hydroxyl groups in the newly formed oxepine structure **13**, the acylated hydroxyl groups have to be liberated before the <sup>31</sup>P NMR analysis. For this purpose the DFRC treated model **1** was hydrolyzed with sodium hydroxide for 24 h at 45–50 °C. Three clear <sup>31</sup>P NMR signals of the same intensity were thus obtained, characteristic of structure **13** (Figure 2).

The <sup>31</sup>P signal of the aliphatic hydroxyl group on the  $\gamma$ -carbon was found at 148.15 ppm and the signal of the phenolic hydroxyl

**Scheme 3.** Formation of Oxepine **13**, from Dibenzodioxocin, **1**, Treated with AcBr in Acetic Acid



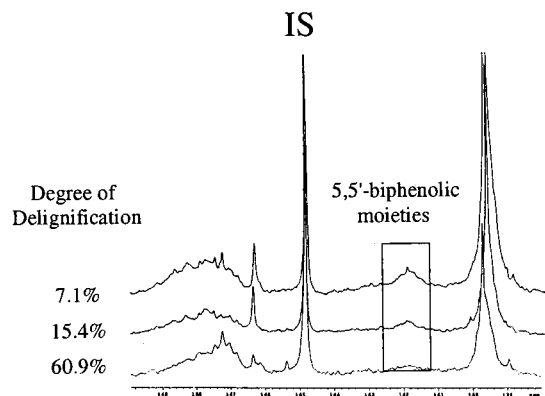


**Figure 3.** Quantitative  $^{31}\text{P}$  NMR spectra of DFRC products from residual lignins, isolated from kraft pulps at various degrees of delignification. The signal intensity at  $\sim 142$  ppm progressively declines as the degree of delignification increases.

group at 139.60 ppm. The newly formed phenolic group was found at 143.18 ppm. This sequence of reactions and our conclusions are depicted in **Scheme 3**. Oxepine **13** was further characterized by a series of detailed 2D NMR experiments, which are described in the Appendix of this paper.

As expected, when we treated **1** with acetic acid at room temperature for 3 h (DFRC temperature regime and time scale), only the starting dibenzodioxocin was recovered. Furthermore, we concluded that during the reductive cleavage stage, the oxepine structure remains intact.

**Reactivity of Dibenzodioxocins in MWL under DFRC Conditions.** Confronted with the described isomerization of dibenzodioxocins to oxepines under DFRC conditions, the objective of ensuing experiments became to determine whether dibenzodioxocin structures embedded within the polymeric structure of lignin undergo similar transformations.

When softwood MWL was treated under DFRC conditions, the reaction apparently proceeded according to **Scheme 2**, as per our original expectations, but contrary to the observed reactions of DBDOX models. We surmise that the reason is due to steric factors imposing rotation restrictions within the lignin macromolecule. The nucleophilic attack of the opened DBDOX ring **A**, at  $\text{C}_2$ , on the carbocation (or alternatively the electrophilic attack of the carbocation on the aromatic ring at  $\text{C}_2$ ) requires considerable bond reorientation to occur. When the side chains are part of the macromolecular structure, and even the aromatic ring **C** is possibly further etherified into lignins, rotation becomes difficult. More specifically, the rotation shown in **Scheme 3** for the transition from **10** to **11** is possible for model compound **1**, but it is not possible in lignin because all three C9 units are anchored to the lignin structure and their movements are restricted. Therefore, after the cleavage of the  $\alpha$ -ether the structure remains open and is not recycled. The released phenolic hydroxyl group becomes acetylated (structure **5**, **Scheme 2**). Although the presence of bromine at the  $\alpha$ -position of **5** was not detected, we assume that this must have occurred to explain the formation of **6** and **7**. This is because during the reductive cleavage step the  $\beta$ -ether bond is cleaved and 5,5'-biphenyl **6** is released as a final product.

After the reductive cleavage step, monoacetylated 5,5'-biphenolic moieties were released (instead of oxepines **13**) as degradation products of the dibenzodioxocin structures. This was initially confirmed by the  $^{31}\text{P}$  NMR spectra, which showed a new signal due to biphenolic moieties centered around 142.0 ppm (from 142.6 to 141.4 ppm). Symmetric 5,5'-biphenolic moieties show a  $^{31}\text{P}$  NMR signal at  $\sim 141.0$  ppm indicative of

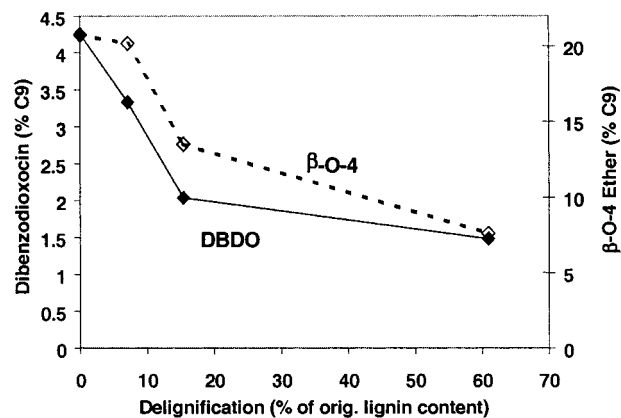


**Figure 4.** Plot showing the progressive reduction of dibenzodioxocins (DBDO) compared to that of arylglycerol- $\beta$ -aryl ethers present in residual kraft lignin as a function of degree of delignification.

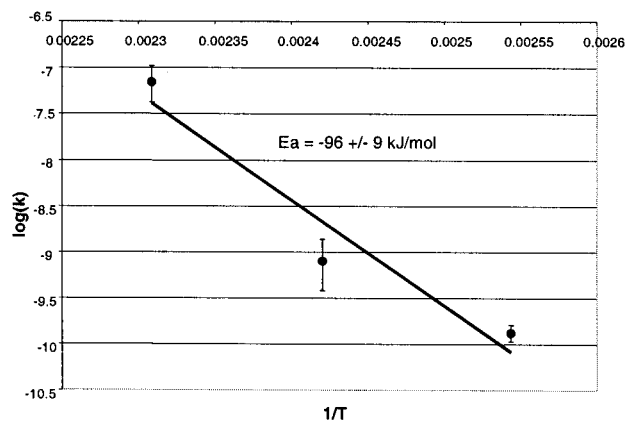


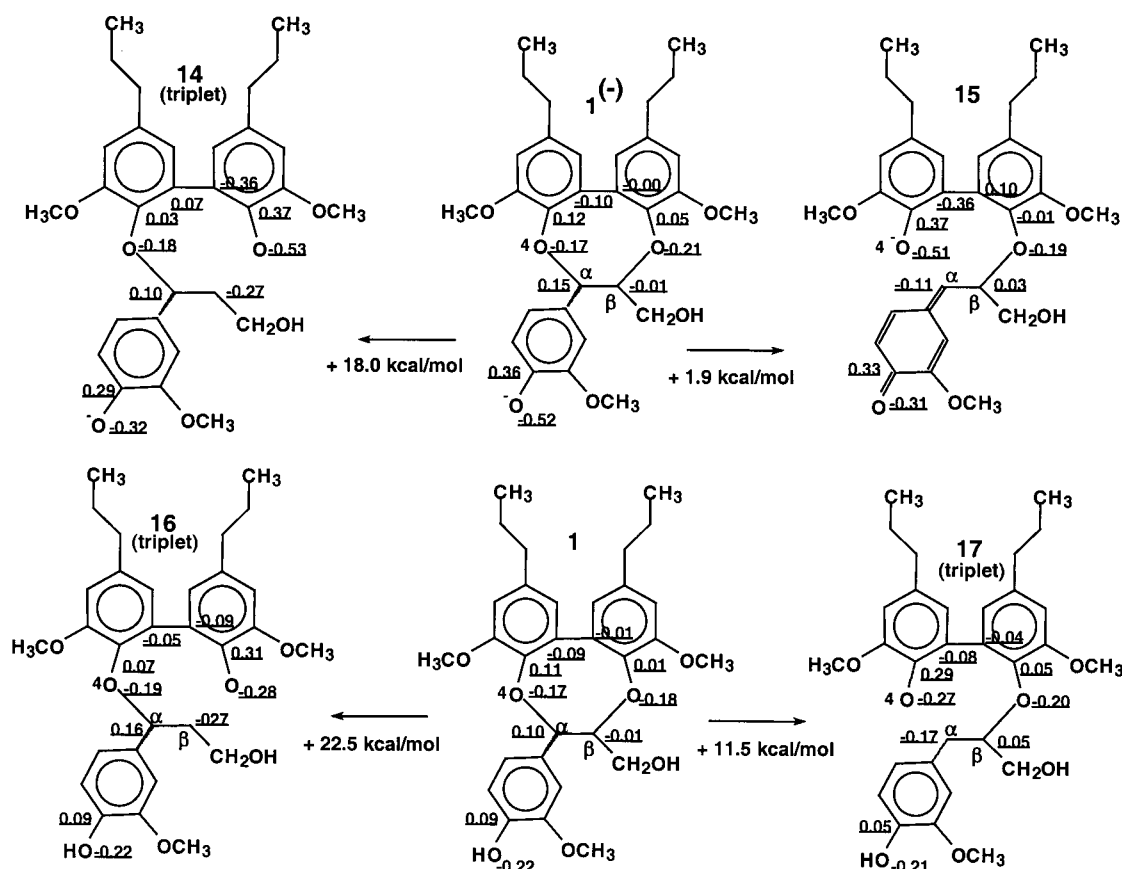
**Figure 5.** Arrhenius plot for the determination of the activation energy for the degradation of a dibenzodioxocin model compound under kraft conditions.

two equivalent phosphitylated phenolic hydroxyl groups. The presence of an acetate on one of the two phenolic moieties (as depicted in **Scheme 2**, structure **6**) is expected to give rise to a phenolic moiety having a  $^{31}\text{P}$  NMR signal shifted downfield by  $\sim 1.0$  ppm (*19*).

In a series of triplicate experiments the amount of phenolic hydroxyl group released in the 5,5'-biphenyl region was determined to be 0.23 mmol/g. Because the 5,5'-biphenyl released from the DFRC treatment of dibenzodioxocin contains only one free phenolic hydroxyl group, this figure is approximately half the amount quantified by the treatment of MWL with alkaline hydrosulfide, discussed in **Figure 1**. These quantitative analyses revealed that 12.9/100 C9 phenylpropanoid units were involved in DBDO structures in softwood milled lignin. This estimate of the dibenzodioxocin abundance is comparable to the 11.1 value obtained from the alkaline hydrosulfide degradation experiments. Therefore, the combination of the DFRC method with quantitative  $^{31}\text{P}$  NMR analysis provides an independent means for the determination of the abundance of dibenzodioxocins in polymeric lignins.

**Rates of Dibenzodioxocin Degradation under Kraft Delignification Conditions.** Using the accumulated information with MWL, we explored further the applicability of the DFRC method for investigating the abundance of dibenzodioxocins in residual kraft lignins isolated from pulps at various degrees of kraft delignification.

As already discussed, kraft pulping cleaves dibenzodioxocins, forming stoichiometric amounts of 5,5'-biphenyl structures.

Scheme 4. Computed Charge Distributions in Dibenzodioxocin Moieties<sup>a</sup>

<sup>a</sup> The charges are underlined. Some atoms are labeled "4", " $\alpha$ ", and " $\beta$ " in keeping with the traditional terminology of wood chemistry.

Consequently, one may expect that the dibenzodioxocin moieties in residual kraft lignin (20) would gradually decrease as delignification proceeds (Figures 3 and 4). When residual kraft lignins were isolated from a series of kraft pulps subjected to different degrees of delignification (with 7.1, 15.4, and 60.9% removal of total lignin), the data of Figure 4 were obtained. The amounts of liberated phenolic hydroxyl groups responsible for dibenzodioxocins and  $\beta$ -O-4 structures are plotted in Figure 4 as a function of degree of delignification.

The data of Figure 4 demonstrate that  $\sim$ 50% of dibenzodioxocin structures are readily cleaved during the kraft pulping process. It is notable that there is a 22% decrease of dibenzodioxocin structures at the onset of delignification (from 0 to 7.1%), whereas only  $\sim$ 2.7% of the arylglycerol- $\beta$ -aryl ether bonds were cleaved within the same delignification interval. This signifies that the dibenzodioxocin moieties are relatively labile, especially at initial phases of kraft delignification. However, in later stages of delignification the overall pattern of dibenzodioxocin removal is similar to that of  $\beta$ -ether linkages.

**Activation Energy for the Degradation of Dibenzodioxocins.** In an effort to further comprehend the data of Figure 4 we conducted a series of experiments aimed at defining the activation energy for the degradation of dibenzodioxocin structures in lignin. We then compared these data to those required for the scission of arylglycerol- $\beta$ -aryl ether bonds under the same conditions.

The degradation of *trans*-6,7-dihydro-7-(4-hydroxy-3-methoxyphenyl)-4,9-dimethoxy-2,11-dipropylidibenzo[*e,g*][1,4]-dioxocin-6-ylmethanol, **1** (Scheme 1), was carried out in alkaline media in the presence of hydrosulfide anions (white liquor, for details see Materials and Methods) at three different

temperatures (120, 140, and 160 °C) as a function of time (ranging from 5 min to 5 h), and the amount of 5,5'-biphenyl **4** released was determined using quantitative HPLC procedures. The derived rate constants were then used for the calculation of the Arrhenius parameters. The error bars apparent in the plot of Figure 5 were computed from the errors of the slopes used to compute the first-order rate constants at various temperatures. The error of the estimate of the activation energy was computed by considering the average errors of these slopes. The activation energy for the degradation of dibenzodioxocin model **1** was determined to be  $-96 \pm 9$  kJ/mol (Figure 5).

As depicted in Scheme 1, under alkaline conditions the  $\alpha$ -O-4 ether bond of compound **1**<sup>(-)</sup> is cleaved at the onset of the reaction, releasing intermediates **2** bearing one phenolate anion and a  $\beta$ -aryl ether quinone methide. Reaction with hydrosulfide anion (HS<sup>-</sup>) yields structure **3** bearing two phenolate anions. The next step in the degradation is  $\beta$ -aryl ether bond scission and liberation of 5,5'-biphenyl **4**. Ahvazi et al. (26) have studied the degradation of arylglycerol- $\beta$ -aryl ether bonds in MWL and observed that the overall reaction of the cleavage of arylglycerol- $\beta$ -aryl ether structures followed a pseudo-first-order rate law. In fact, the degradation proceeded in two phases. The activation energy for the fast initial phase was determined to be  $-40.9$  kJ/mol, whereas the activation energy for the slower bulk phase was  $-117.5$  kJ/mol. The activation energy for the dibenzodioxocin model compound **1** studied here is closer to the figure obtained by Ahvazi et al. for the bulk reaction (26).

**Computational Characterization of the Dibenzodioxocin Ether Bonds.** The  $\alpha$ -O-4 ether bond is prominently involved in many reactions of dibenzodioxocin compounds. Scheme 4 shows two types of such compounds, compound **1**, in which

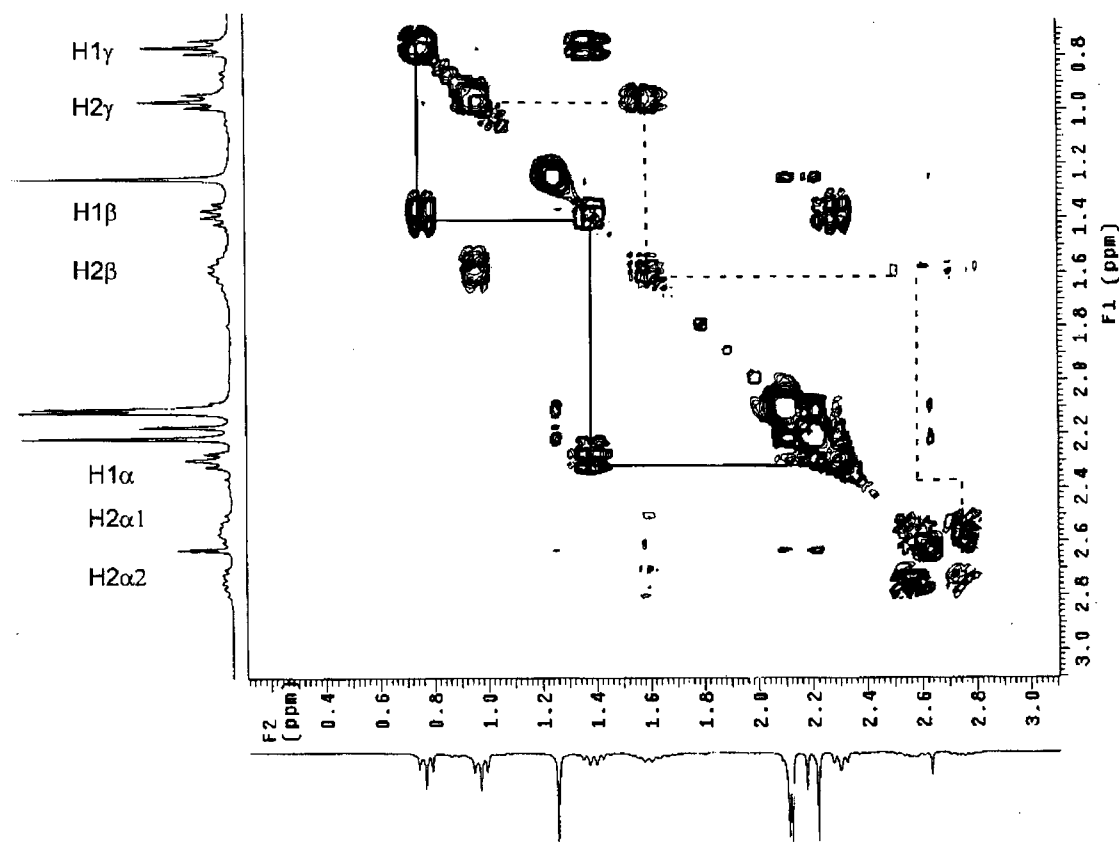


Figure 6. Part of the 2D COSY spectrum of **13**. Continuous lines represent an AMX spin system and the dotted lines an AMXY spin system.

the free hydroxyl is protonated, and **1**<sup>(-)</sup>, in which this group is ionized. Charge distribution calculations for these molecules show striking differences in the vicinity of the phenolic groups, between the highly polarized C–O bond of compound **1**<sup>(-)</sup> (charges 0.36 and –0.52) and the much less polarized C–O bond of compound **5** (charges 0.09 and –0.22). The charge distribution in the rest of the structures depicted in **Scheme 4** is rather similar. However, if the  $\alpha$ -O-4 bonds of structures **1**<sup>(-)</sup> and **1** are cleaved, yielding structures **15** and **17**, respectively, the charge distribution patterns change considerably. The phenolate **15** now acquires high polarity (charges 0.37 and –0.51) on the C–O bond corresponding to the former  $\alpha$ -O-4 ether bond. These charges are quite similar to those previously detected on the phenolate group of **1**<sup>(-)</sup>, indicating that the phenolate “migrated” to a new position. Thus, a quinone methide structure drawn for structure **15** is a more appropriate interpretation of the new charge distributions. The polarity of the C=O bond (charges 0.33 and –0.31) of the quinone moiety **15** is intermediate between the phenolate **1**<sup>(-)</sup> and the phenol **1**.

When a similar bond dissociation is performed on **1**, the  $\alpha$ -O-4 bond is also broken and the ensuing structure **17** acquires a new charge distribution. The polarity of the C–O bond (charges 0.29 and –0.27) corresponding to the former  $\alpha$ -O-4 ether bond is now similar to that of the aforementioned quinone bond. Another major change in charge distribution occurred on the carbon, making it similar to the double-bonded  $\alpha$  carbon of the quinone moiety of structure **17**. The charge distributions suggest that if the  $\alpha$ -O-4 bond is broken, the ether oxygen becomes phenolate-like in compound **15** and quinone-like in structure **17**.

The transition of the phenolate dibenzodioxocin compound **1**<sup>(-)</sup> into a quinone methide **15** is an endothermic transformation requiring 1.9 kcal/mol. The  $\alpha$ -O-4 bond is broken in the process, and the geometries of the two forms must be quite different. In

view of the relatively low heat of this transition and considering likely that the entropy of the quinone methide form is higher (due to free rotation around the  $\beta$ -O-4 bond), it is possible that, albeit slightly endothermic, the transformation can run spontaneously. Thus, the  $\alpha$ -O-4 bond in the dibenzodioxocin compounds with free phenolic group might break spontaneously under alkaline conditions. The  $\alpha$ -ether bond of the protonated form of dibenzodioxocin, **1**, appears to be stronger (dissociation energy + 11.5 kcal/mol) than in **1**<sup>(-)</sup>.

Computations of the dissociative bond energies for the  $\beta$ -ether bonds in dibenzodioxocin structures show that the energies are higher than in the  $\alpha$ -ether bonds, suggesting a higher stability of the  $\beta$ -ethers. Unlike the  $\alpha$ -ether bonds, the  $\beta$ -ether bond in the anionic dibenzodioxocin model **1**<sup>(-)</sup> is only slightly smaller (18 kcal/mol) than in the protonated model **1** (22.5 kcal/mol), suggesting that the  $\beta$ -ether bond lability is not affected by the ionization state as much as the  $\alpha$ -ether bond is.

The results of the computations are consistent with the degradation schemes in which reactions of dibenzodioxocin structures in both alkaline and acid conditions are always initiated by the cleavage of the  $\alpha$ -ether bond.

#### ACKNOWLEDGMENT

We thank Dr. John Ralph of the U.S. Dairy Forage Research Centre, USDA-ARS, Madison, WI, and Dr. Jean Bouchard of Paprican for the constructive review offered to us during the preparation of the manuscript.

#### APPENDIX

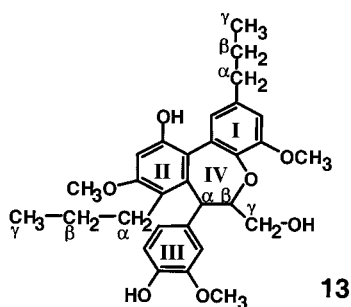
**2D NMR Experiments on Oxepine 13.** The following NMR study for the structural verification of **13** was carried out to identify it as 11-hydroxy-7-(4-hydroxy-3-methoxyphenyl)-6-hy-

**Table 1.** Chemical Shift Values (Parts per Million) for the Side-Chain Protons

	CH <sub>3</sub> ( $\gamma$ )	CH <sub>2</sub> ( $\beta$ )	CH <sub>2</sub> ( $\alpha$ 1/ $\alpha$ 1)
aromatic ring I	0.76	1.38	2.30
aromatic ring II	0.96	1.59	2.56/2.75

**Table 2.** Chemical Shift Values (Parts per Million) of Ring IV Proton and Carbon Signals

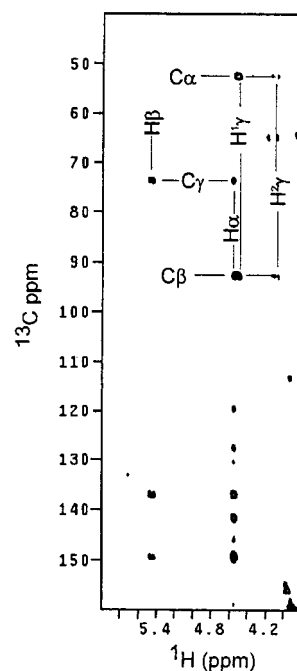
	CH( $\alpha$ )	CH( $\beta$ )	CH <sub>2</sub> ( $\gamma$ 1/ $\gamma$ 2)
proton signals	4.52	5.40	4.06
carbon signals	52.8	93.1	74.2

**Scheme 5.** Labeling of the Oxepine Structure Obtained from the NMR Analyses

droxymethyl-4,10-dimethoxy-2,8-dipropyl-6,7-dihydrodibenzo-*[b,d]*oxepine.

**Spectral Assignments. Aromatic Side Chains.** Together with the integration values of a proton 1D spectrum collected with a long relaxation delay, A3M2X2 (continuous lines) and A3M2XY (dotted lines) spin systems are clearly identified in the upfield region (0–3 ppm) in the 2D COSY map (see **Figure 6**) This uniquely identifies the two CH<sub>3</sub>( $\gamma$ )–CH<sub>2</sub>( $\beta$ )–CH<sub>2</sub>( $\alpha$ ) side chains in structure **13**. Between these two side chains, the one which is bonded to the aromatic ring II has the possibility of restricted rotations about the bond C $\alpha$ –C (aromatic ring), and as a result two  $\alpha$ -protons are magnetically nonequivalent. Assignments of the two side-chain protons are listed in **Table 1**.

**Ring IV Proton/Carbon Assignments.** From the 2D COSY map, an AMX spin system was identified in the region between 4 and 6 ppm (data not shown). 1D TOCSY traces of selective excitation of the multiplets at 5.4 ppm at several values of spin locking time between 15 and 150 ms (not shown) further extended this spin system to an AMPX. Integration of the proton 1D spectrum indicates one proton intensity for each spin species. Their characteristic chemical shift values and the spin coupling pattern therefore uniquely identify this spin system as belonging to the ring IV protons. Further assignments of all proton and carbon signals can be obtained from the heteronuclear correlation 2D experiments. C $\gamma$  and H $\gamma$ s can be easily identified from the HMQC spectrum because they uniquely show two cross-peaks along the C $\gamma$  frequency. This assignment will lead to the identification of H $\beta$  and C $\beta$  from the COSY and HMQC maps. The left spin species will naturally be the H $\alpha$  and C $\alpha$  signals. All of the proton and carbon assignments were further corroborated with an HMBC experiment, in which a low-pass filter is inserted in a conventional HMQC experiment and therefore allows the remote carbon–proton coupling observable. A summary of key connections is summarized in the HMBC map (**Figure 7**), and the chemical shift values are listed in **Figure**

**Figure 7.** HMBC subspectrum of **13** showing the long-range carbon–proton correlations for oxepine ring IV.

7. As anticipated, both H $\alpha$  and H $\beta$  show cross-peaks to aromatic carbons, with H $\alpha$  extended further away (**Figure 7**). The lack of H $\alpha$ /H $\beta$  and H $\beta$ /C $\alpha$  could be due to an unfavorable geometric arrangement leading to an unusual small *J* coupling.

#### LITERATURE CITED

- (1) Argyropoulos, D. S.; Menachem, S. B. Lignin. In *Advances in Biochemical Engineering/Biotechnology*; Eriksson, K.-E., Ed.; Springer-Verlag: Berlin, Germany, 1997; Vol. 57, pp 127–158.
- (2) Sakakibara, A. A Structural Model of Softwood Lignin. *Wood Sci. Technol.* **1980**, *14*, 89–100.
- (3) Lundquist, K. Wood. In *Methods in Lignin Chemistry*; Lin, S. Y., Dence, C. W., Eds.; Springer-Verlag: Berlin, Germany, 1992; pp 65–70.
- (4) Argyropoulos, D. S. Applications of Quantitative <sup>31</sup>P NMR to Pulping, Bleaching and Yellowing. In *Advances in Lignocellulose Characterization*; Argyropoulos, D. S., Ed.; Tappi Press: Atlanta, GA, 1999; pp 109–129.
- (5) Gierer, J. Chemistry of Delignification. Part I: General Concept and Reactions During Pulping. *Wood Sci. Technol.* **1985**, *12*, 289–312.
- (6) Berthold, F.; Lindfors, E.-L.; Gellerstedt, G. Degradation of Guaiacylglycerol- $\beta$ -3-Guaiacyl Ether in the Presence of HS- or Polysulphide at Various Alkalinities. Part I. Degradation Rate and the Formation of Enol Ether. *Holzforchung* **1998**, *52*, 398–404.
- (7) Freudenberg, K. Entwurf eines Konstitutionsschemas für das Lignin der Fichte. *Holzforchung* **1964**, *18*, 3–9.
- (8) Eriksson, M.; Larsson, S.; Miksche, G. E. Gas-Chromatographic Analysis of Lignin Oxidation Products. VII. An Improved Characterization of Lignins through Methylation and Oxidative Decomposition. *Acta Chem. Scand.* **1973**, *27*, 127–140.
- (9) Pew, J. C. Evidence of a Biphenyl Group in Lignin. *J. Org. Chem.* **1963**, *28*, 1048–1054.
- (10) Drumond, M.; Ayoama, M.; Chen, C.-L.; Robert, D. Substituent Effects on C-13 Chemical Shifts of Aromatic Carbons in Biphenyl Type Lignin Model Compounds. *J. Chem. Wood Technol.* **1989**, *9*, 421–441.
- (11) Argyropoulos, D. S. Quantitative Phosphorus-31 NMR Analysis of Six Soluble Lignins. *J. Wood Chem. Technol.* **1994**, *14* (1), 65–82.

- (12) Li, S.; Lundquist, K. New Method for the Analysis of Phenolic Groups in Lignin by  $^1\text{H-NMR}$  Spectrometry. *Nordic Pulp Paper Res. J.* **1994**, *9* (3), 191–195.
- (13) Karhunen, P.; Rummakko, P.; Sipila, J.; Brunow, G.; Kilpelainen, I. Dibenzodioxocins; A Novel Type of Linkage in Softwood Lignins. *Tetrahedron Lett.* **1995**, *36*, 169–170.
- (14) Karhunen, P.; Rummakko, P.; Pajunen, A.; Brunow, G. Synthesis and Crystal Structure Determination of Model Compounds for the Dibenzodioxocin Structure Occurring in Wood Lignins. *J. Chem. Soc., Perkin Trans. 1*, **1996**, 2303–2308.
- (15) Adler, E. Lignin Chemistry—Past, Present and Future. *Wood Sci. Technol.* **1977**, *11*, 169–218.
- (16) Lapierre, C.; Monties, B.; Rolando, C. Thioacidolysis of Lignin: Comparison with Acidolysis. *J. Wood Chem. Technol.* **1985**, *5* (2), 277–292.
- (17) Lu, F.; Ralph, J. DFRC Method for Lignin Analysis. 1. New Method for  $\beta$ -Aryl Ether Cleavage: Lignin Model Studies. *J. Agric. Food Chem.* **1997**, *45*, 2590–2592. Lu, F.; Ralph, J. Reactions of Lignin Model  $\beta$ -aryl Ethers with Acetyl Bromide. *Holzforschung* **1996**, *50* (4), 360–364.
- (18) Tohmura, S.; Argyropoulos, D. S. Determination of arylglycerol- $\beta$ -aryl ether and other linkages in lignins using DFRC/ $^{31}\text{P}$  NMR. *J. Agric. Food Chem.* **2001**, *49*, 536–542.
- (19) Jiang, Z. H.; Argyropoulos, D. S.; Granata, A. Correlation Analysis of  $^{31}\text{P}$  NMR Chemical Shifts with Substituent Effects of Phenols. *Magn. Reson. Chem.* **1995**, *33*, 375–382.
- (20) Stewart, J. J. P. Optimization of Parameters for Semiempirical Methods. I. Method. *J. Comput. Chem.* **1989**, *10* (2), 209–220.
- (21) Stewart, J. J. P. Optimization of Parameters for Semiempirical Methods. II. Applications. *J. Comput. Chem.* **1989**, *10* (2), 221–264.
- (22) Jurasek, L.; Argyropoulos, D. S. A Detailed Study of the Alkaline Oxidative Degradation of A Residual Kraft Lignin Model Compound. In *Oxidative Delignification Chemistry: Fundamentals and Catalysis*; ACS Symposium Series 785; Argyropoulos, D. S., Ed.; American Chemical Society: Washington, DC, 2001; pp 130–148.
- (23) Karhunen, P. Studies on Synthesis and Reactions of Lignin Model Compounds with Biphenyl, Diaryl Ether and Dibenzodioxocin Structures. Academic Dissertation, University of Helsinki, 1999.
- (24) Granata, A.; Argyropoulos, D. S. 2-Chloro-4,4,5,5-tetramethyl-1,3,2-dioxaphospholane a Reagent for the Accurate Determination of the Uncondensed and Condensed Phenolic Moieties in Lignins. *J. Agric. Food Chem.* **1995**, *43*, 1538–1544.
- (25) Brunow, G. Oxidative Coupling of Phenols and the Biosynthesis of Lignin. In *Lignin and Lignan Biosynthesis*; Lewis, N. G., Sarkanen, S., Eds.; American Chemical Society: Washington, DC, 1998; pp 131–147.
- (26) Ahvazi, B. C.; Argyropoulos, D. S. Thermodynamic parameters governing the stereoselective degradation of arylglycerol- $\beta$ -aryl ether bonds in milled wood lignin under kraft pulping conditions. *Nordic Pulp Pap. Res. J.* **1997**, *12* (4), 282–288.

---

Received for review July 12, 2001. Revised manuscript received November 14, 2001. Accepted November 14, 2001.

JF010909G